Novel Cellulose Nanofibers/Polyvinyl Alcohol/Polyethyleneimine Nanoparticle for Cu^{2+} Removal in Water

Rongrong Si
QLUT: Qilu University of Technology
Chaojun Wu (Chaojunwu2007@163.com)
Qilu University of Technology https://orcid.org/0000-0002-7840-0077
Dongmei Yu
Qilu University of Technology
Qijun Ding
Qilu University of Technology
Ronggang Li
Qilu University of Technology

Research Article

Keywords: Cellulose nanofibers, nanoparticle, heavy metal ions, adsorption

Posted Date: May 13th, 2021

DOI: https://doi.org/10.21203/rs.3.rs-485817/v1

Abstract

In this study, environmentally friendly CNF/PVA/PEI nanoparticle was obtained by assembling PEI (polyethyleneimine) into CNF/PVA aerogels, which were prepared by freeze-drying method with the help of glutaraldehyde. FTIR results showed that PEI likely assembled into the CNF/PVA aerogel due to appearances of bending vibration of the CNF/PVA/PEI nanoparticle at 1615cm^{-1}. BET results further demonstrated that PEI have successfully assembled into aerogel since the specific surface area (22.93m^2/g) of CNF/PVA/PEI nanoparticle was lower than that (56.37m^2/g) of CNF/PVA aerogel. SEM results also showed that PEI could obviously regulate the morphology of CNF/PVA aerogel. TGA indicated that CNF/PVA/PEI nanoparticle was structurally stable at 216.4°C. The adsorption kinetics of the CNF/PVA/PEI nanoparticle for Cu^{2+} removal presented good correlations with the Pseudo-second-order model. The adsorption and desorption results showed that the removal rate of 2g/L CNF/PVA/PEI nanoparticle for Cu^{2+}in water could reach more than 93% when the concentration of Cu^{2+} ranged from 20 to 80mg/L in one hour, and it could still retain more than 80% after 3 cycles.

Introduction

Nowadays, with the rapid growing of economic and industrialization, heavy metal ions has been the most serious problem in water environment due to their toxicity and incompatibility(Fu and Wang 2011). Heavy metal ions,such as copper (Cu)(II) ,hydrargyrum(Hg)(II), chromium (Cr)(VI), plumbum (Pb)(II) and so on have posed a great threat to human survival due to its undegradability and toxicity in water(Uddin 2017).

There are many traditional methods to solve the problems caused by heavy metal ions, such as adsorption, coagulation, membrane separation, oxidation and ion exchange(Wan Ngah and Hanafiah 2008). Among them, adsorption is considered to be one of the most popular strategies for heavy metal ion removal because of the high removal efficiencies, flexibility in the design and application of adsorbents, and low cost(Qin et al. 2019).The adsorbents mainly include activated carbon, clay, biochar and polymers. Recently, nanocellulose based adsorbents become more and more popular as nanocellulose has higher specific surface area, excellent mechanical properties and good biocompatibility(Du et al. 2016; Jordan et al. 2019).

It is reported that the heavy metal Cu^{2+}usually accumulates in human liver and cause serious anemia and hemolysis(Stern 2010).Tang et al.(2020a) used 3-glycidyloxypropyl) trimethoxy silane (GPTMS) as a cross-linking agent to cross-link PEI onto the cellulose nanofibril skeleton and quickly freeze-dried with liquid nitrogen to obtain aerogel beads. Its maximum adsorption capacity for Cu^{2+}reached 163.4mg/g. Zhang et al.(2016) used glutaraldehyde as a cross-linking agent to cross-link PEI onto TOCN and then freeze-dried to obtain TOCN-PEI adsorbent with a maximum adsorption capacity of 52.32 mg/g for Cu^{2+}.Mo et al.(2019) used Trimethylolpropane-tris-(2-methyl-1-aziridine) propionate (TMPTAP)as a cross-

linking agent and cross-linked PEI and TO-CNF to obtain TO-CNF/TMPTAP/PEI aerogel. Its maximum adsorption capacity of Cu^{2+}could reach 485.44mg/g.

It was reported that PVA could be used as environmentally friendly adsorption material due to its good biocompatibility and biodegradability (Niu et al. 2018; Zheng et al. 2014). In this study, we prepared CNF/PVA/PEI nanoparticle through a freeze-drying method. The structures and properties of CNF/PVA/PEI nanoparticle were analyzed by FTIR, SEM, TGA and fully automatic gas adsorption analyzer. The adsorption performance of CNF/PVA/PEI nanoparticle on Cu^{2+} was investigated, and its reusability was also being explored.

Experimental

Material and methods

Materials: Bleached softwood pulp(BSP, Shandong Province, China)，2,2,6,6-Tetramethylpiperidine 1-oxyl(TEMPO, Shanghai, Aladdin.) ，NaBr (AR grade)，sodium hypochlorite (NaClO) solution (regent grade, 10-15% chlorine)，polyvinyl alcohol(PVA, alcoholics degree/mol ≥97%)，polyethyleneimine(PEI,70000Mw), sodium hydroxide (NaOH, AR grade), cooper(II) nitrate ($Cu(NO_3)_2$), glutaraldehyde (GA, 50% in water)，

Preparation of TEMPO-oxidized cellulose nanofibers.

The TEMPO oxidized cellulose nanofibers(TOCNF) were prepared according to previously reported methods(Qin et al. 2011). Weigh 4gBSP accurately, disperse in 400ml deionized water, add 0.016g TEMPO, 0.16g NaBr, 80ml 10% NaClO solution. After that, 0.1MHCl was used to adjust the optimal pH to 10-10.4. In the reaction process, the pH of the solution will gradually decrease with the formation of carboxyl group. 0.5MNaOH solution is used to adjust the pH to 10 until the pH no longer drops, and 5mL ethanol is used to terminate the reaction.

Preparation of TOCNF/PVA aerogel

The PVA solution (12.5mL, 8wt%), CNF solution (100g, 1wt%) were mixed together in a flask under vigorous stirring for 4h. The weight ratio between the PVA and CNF were 1:1(Zheng et al. 2014).At the final stage, CNF/PVA solution was placed for 24h to remove bubbles. The freeze-drying process was maintained at -30°C to obtain CNF/PVA aerogel.

Preparation of CNF/PVA/PEI nanoparticle

Add 2g CNF/PVA aerogel into 100ml 10% PEI/methanol (w/v) solution and stir at 30°C for 24h. Then wash with methanol to remove unreacted PEI. Then disperse the precipitate in 100mL deionized water, then slowly add 4mL of 25% glutaraldehyde aqueous solution, then adjust the pH to 8 with 0.4M NaOH. Stir for one hour to make the two react, and finally, wash the product with deionized water and freeze Dry to obtain CNF/PVA/PEI adsorbent.

Characterization

FTIR

Fourier transform infrared spectroscopy (IR Prestige21 Shimadzu Corporation) spectra were obtained using the Alpha infrared spectrometer with a scanning number of 32 from 250 to 4250 cm^{-1}.

SEM

Scanning electron microscope (Regulus 8220, Japan) was used to characterize the morphology of materials. All the specimens were coated with Au before observation.

TGA

Thermogravimetric analysis (TGA) was conducted with a synchronous thermal analyzer (STA449, USA) test. Samples were heated at a constant heating rate of 10°C/min, from room temperature (RT) to 650°C, under inert (N_2) atmosphere.

BET

The specific surface aeras were measured by the Brunauer–Emmett–Teller (BET) method based on N_2 adsorption. The determinations were carried out from freeze-dried samples with an analyzer (Micromeritics, USA). Prior to testing, the samples should be degassed at 120°C for 4h.

Adsorption experiments

The initial concentrations of Cu^{2+} was set to be 1000mg/L. The whole contact time was 2 h under Temersionoxcillator registration (Noki)at room temperature for all batch experimental process. Residual concentration of Cu^{2+} were measured by flame atomization atomic absorption spectrometry (AAS, GGX-600, China). The amount of Cu^{2+} adsorbed onto the adsorbent was calculated from the difference between the initial (C_0) and the remaining (Ce) metal concentration in solution(Anirudhan et al. 2019).

$$\text{Removal rate } (\%) = \frac{C0-Ce}{C0} \times 100\%$$

Where C_0 is the initial concentration of Cu^{2+}(mg/L) and Ce is the concentration of Cu^{2+} at equilibrium time.

Adsorption kinetics

The known Pseudo-first-order kinetics, Pseudo-second-order kinetics, Intra-particle diffusion model and Elovich equation are commonly used for describing the adsorption mechanism of heavy metal ions. For the first-order model, the adsorption is controlled by diffusion and mass transfer of the adsorbate to the

adsorption site(A et al. 2017). For the Pseudo-second-order model, chemisorption is the rate-limiting step. The linearized forms of these equations were expressed as follows(Islam et al. 2017; Pal et al. 2017):

$$\ln(Q_0 - Q_t) = \ln Q_0 - K_1 t$$

$$\frac{t}{Q_t} = \frac{1}{k_2 Q_0^2} + \frac{t}{Q_0}$$

$$Q_t = k_i t^{0.5} + C$$

$$Qt = A + k_e lnt$$

where Qt is the adsorption capacity after time t and Q_0 is the saturated adsorption capacity of Cu^{2+}; k_1 and k_2 are the constants of the first-order and second-order kinetics respectively; ki and C are the constants of the Intra-particle diffusion model; ks and A are the constants of the Elovich equation.

The effect of pH on adsorption capacity

The initial pH value of the copper solution has a crucial influence on the absorption performance of the absorbent, because it determines the form of the copper ion species and the electrostatic repulsion between the absorbent and Cu^{2+} ions. Due to the presence of amino groups in CNF/PVA/PEI, the surface charge will change with the change of pH, thereby affecting the adsorption capacity. In addition, when the pH exceeds 6.5, Cu^{2+} ions may be converted to $Cu(OH)_2$ precipitation(Shao et al. 2017), it may cause deviations in the adsorption process. Therefore, the pH of the solution is set to 2, 3, 4, 5, 6. The sample is 0.05g. Take 50ml of 20mg/L Cu^{2+} ion standard solution and adjust the pH to 2, 3, 4, 5, and 6, respectively. A sodium hydroxide aqueous solution (NaOH, 0.1mol/L) was used for pH adjustments.

The effect of adsorption time on adsorption capacity

Take 0.1g sample and add it to the copper ion solution with pH 6, the concentration is 20mg/L, the sampling time is 10, 20, 30, 60, 120, 180, 240 minutes to determine the time required for adsorption to reach equilibrium.

Adsorption experiments

The standard solution of Cu^{2+} is dispersed in deionized water for later experiments (20, 40, 60, 80 mg/L for adsorption experiments and thermodynamic curve study). 0.1g CNF/PVA/PEI nanoparticle were added to 50ml Cu^{2+} solution. Shake in a constant temperature shaking box for 24 hours at a temperature of 25°C, then take the supernatant and determine the adsorption capacity with an atomic absorption analyzer to determine the adsorption capacity.

Desorption experiments

The 100mg CNF/PVA/PEI nanoparticle adsorbed with Cu^{2+} were dispersed in 1M HCl solution and stirred at room temperature for 1 hour to remove Cu^{2+}ions. The nanoparticle was then submerged into deionized water to remove the excess acid until the pH reached 7, and the nanoparticle were dried for the next adsorption process.

Results And Discussions

Crosslinking types in CNF/PVA aerogel and CNF/PVA/PEI nanoparticle

It is clear that softwood bleached pulp cellulose has absorption peaks at 3400cm^{-1}, 1430cm^{-1}, 1370cm^{-1}, 1322cm^{-1} and 897cm^{-1}(Fig.1), which are O-H group stretching vibration, C-H scissoring vibration, C-H bending vibration, O-H in -plane vibration and C-H deformation vibration of cellulose, respectively(Zhu et al. 2021). (Sirvio et al. 2015; Tarchoun et al. 2019).It can be observed that TO-CNF appears an intense peak in 1606cm^{-1}, which was assigned to the characteristic peak of the carbonyl of the carboxylic acid group.

Compared with CNF, a absorption peak belonging to PVA appeared at 850cm^{-1} of CNF/PVA aerogel, it may be caused by the formation of intermolecular hydrogen bonds(Takeno et al. 2020). And for CNF/PVA/PEI nanoparticle, the peak in the 1600-1800cm^{-1} region appeared to be the overlap the three individual peaks, which belonged to N-H bending vibration (1615cm^{-1}), C=O stretching vibration for-COO- (1660cm^{-1}) and for -COOH (1713cm^{-1}), respectively. At the peak of 1660cm^{-1}, there is also a C=N group stretching, which appears in the process of glutaraldehyde crosslinking. In addition, at 2923cm^{-1} and 2848cm^{-1} as early as- CH_2—stretching vibrations can also prove that PEI likely assembled into the CNF/PVA aerogel by N-H bond(Tang et al. 2020b).

Morphological analysis of CNF, CNF/PVA aerogel and CNF/PVA/PEI nanoparticle

The morphology and structure of BSP, CNF suspension is dispersed on mica flakes, CNF aerogel, CNF/PVA aerogel and CNF/PVA/PEI nanoparticle were examined by SEM(Fig.2.) The overall and local fiber morphology of bleached softwood pulp was observed at 1K and 60K, respectively. It can be clearly seen that the length of cellulose fiber is about 20-30 microns, and the length can reach vertical microns. SEM results show that there are some pores with diameter of 10-20nm on the surface of cellulose. The CNF obtained by homogenizing after TEMPO oxidation has a diameter between 10-50nm and a length of a few microns. It can be seen that CNF has an excellent aspect ratio, which can have a positive effect on subsequent adsorption(Garba et al. 2020). CNF aerogel and CNF/PVA aerogel were observed at 30 times, and honeycomb structure was found on the surface of CNF aerogel, and porous structure was found on the surface of CNF/PVA aerogel. The CNF/PVA aerogel obtained by freeze-drying after being compounded with PVA has a porous network structure on the surface, which provides a larger area for the cross-linking of PEI. Under the action of glutaraldehyde cross-linking agent, PEI is cross-linked on CNF/PVA aerogel, resulting in a change in the morphology of CNF/PVA/PEI. Specifically, due to the recombination of PEI on the surface of the CNF/PVA aerogel during the GA cross-linking process, the

surface becomes denser and many granular nanoparticle are produced. Nano Measurer Software was used to count the particle size distribution of CNF/PVA/PEI nanoparticle. According to the calculation, the particle size of CNF/PVA/PEI nanoparticle was mainly distributed between 40 and 80nm, accounting for 83% of the total. These phenomena indicate that PEI plays a great role in changing the surface morphology during the cross-linking process.

Thermal stability of CNF, CNF/PVA aerogel and CNF/PVA/PEI nanoparticle

The thermal degradation profiles of BSP, CNF, CNF/PVA aerogel, CNF/PVA/PEI nanoparticle, were assessed by thermogravimetric analysis (TGA) under nitrogen atmosphere from RT (room temperature) to 650°C (Fig.3. a). During the process from RT to 100°C, due to the loss of water, the three substances have a slight quality degradation (not more than 2%)(Eun et al. 2020; Rani et al. 2014). BSP loses the fastest weight in 280°C-399°C, which is the main stage of cellulose pyrolysis. Within this range, BSP is pyrolyzed into small molecular gases and condensable volatiles of macromolecules, resulting in significant weight loss, and its weight loss rate reaches its maximum at about 384.9°C. The maximum degradation temperature of CNF is 320°C (about 50% loss), which is used for the pyrolysis of the cellulose skeleton(Yao et al. 2017). At the end of the analysis, the mass percentage of CNFs pyrolysis residue was 26%. The CNF/PVA aerogel begins to show its first decline at 221.8°C, and the maximum degradation temperature (loss of ca. 40%) appears at about 324.7°C. CNF/PVA/PEI nanoparticle have their first degradation at 216.4°C, and the maximum degradation temperature is 327.5°C (loss of ca. 52%). At the end of the analysis, the remaining CNF/PVA aerogel and CNF/PVA/PEI nanoparticle were 31% and 16%, respectively. The thermal stability of the adsorbents up to 205°C can be a valuable asset in the industrial sector context where the effluents can be warm or hot(Silva et al. 2020).

Specific surface aera of CNF, CNF/PVA aerogel and CNF/PVA/PEI nanoparticle

In order to better explore the morphological evolution of CNF/PVA/PEI nanoparticle, CNF aerogels, CNF/PVA aerogels and CNF/PVA/PEI nanoparticle obtained by freeze-drying CNF suspension were measured. Fig.3(b) shows the N_2 adsorption-desorption curve of the sample at a temperature of 77K. The curve of CNF/PVA/PEI nanoparticle shown in the figure is type 4, which also verifies that the nanoparticle have a mesoporous structure(Wang et al. 2019). As can be seen from Table 1, the BET specific surface area of CNF aerogel is 35.52m^2/g, and the BET specific surface area of CNF/PVA aerogel obtained by freeze-drying after being compounded with PVA solution is 56.37m^2/g, and the specific surface area is greatly increased. After PEI modification, the specific surface area decreased, and the BET specific surface area of CNF/PVA/PEI nanoparticle became 22.93m^2/g, which indicated that PEI was successfully assembled into the CNF/PVA aerogel.

Effect of pH on Cu^{2+}adsorption

As shown in the Fig. 4. (a), the removal rate of CNF/PVA/PEI nanoparticle measured under five different pH conditions of 2, 3, 4, 5, 6. The removal rate CNF/PVA/PEI nanoparticle to Cu^{2+} increased with the

increase of pH value. Due to the protonation of the amino group, it exhibits a lower adsorption capacity at a lower pH. When the pH is 6, the removal rate increased to maximum value (56.55%), so the pH is 6 to learn the adsorption performance of CNF/PVA/PEI nanoparticle.

As shown in the Fig.4. (b), at the beginning, the adsorption capacity increased rapidly and then the increasing trend became slow and finally stabilized, which may be due to the reduction of effective adsorption sites. Therefore, 120min is selected as the best adsorption time for Cu^{2+}.

Fig.4. (c-e) show digital photographs of the Cu^{2+} adsorption in 20mg/L of the adsorbent. Firstly, 0.1gCNF /PVA/PEI nanoparticle are placed in Cu^{2+} solution, and the particles will be suspended in water. After adsorption, the particles will gradually settle at the bottom, which is conducive to the determination of Cu^{2+} and the recycling of CNF/PVA/PEI nanoparticle.

As shown in Fig.4. (b), at four different concentrations, the adsorption equilibrium was reached within two hours, and the removal rates in solutions of 20, 40, 60, and 80 mg/L were 94.1%, 93.6%, 95.7%, and 96.5%, respectively. All are above 93% This indicates that CNF/PVA/PEI nanoparticle may be an excellent adsorbent.

Adsorption kinetics of Cu^{2+} by the CNF/PVA/PEI nanoparticle.

Adsorption kinetics could be used to describe the adsorption mechanism (Fig.4.(b)). It shows the time-dependent adsorption performance of CNF/PVA/PEI nanoparticle at concentrations of 20mg/L, 40mg/L, 60mg/L, and 80mg/L. The adsorption equilibrum was achieved after 1 hours for all 4 concentrations. At four different concentrations, the removal rate of Cu^{2+} ions by CNF/PVA/PEI nanoparticle reached more than 93%. This indicates that CNF/PVA/PEI nanoparticle may become a good adsorption material for removing Cu^{2+} ions from aqueous solutions.

Four curve models, Pseudo-first-order kinetics, Pseudo-second-order kinetics, Intra-particle diffusion model and Elovich equation, are used to explain the adsorption mechanism of Cu^{2+} in aqueous solution. The Table 4andFig.5. (a-d) show the fitted curve and result, respectively. At four different concentrations, the correlation coefficient (R^2s) of the Pseudo-second-order model is all above 0.99. However, for the Pseudo-first-order model, the R^2s is between 0.9006-0.9677. The fitting results of the Intra-particle diffusion model are not very good, and the R^2s of the four concentrations are all less than 0.87. For the fitting results of Elovich equation, the R^2s of the four concentrations are between 0.8065-0.9594. Therefore, the Pseudo-second-order model is considered to be the most suitable data for experimental results. In the adsorption process, both physical adsorption and chemical adsorption exist. The chemical adsorption of Cu^{2+} is a rate-limiting process. Functional groups such as hydroxyl and amino groups in CNF/PVA/PEI nanoparticle provide adsorption sites for chemical adsorption. Large specific surface area will provide more opportunities for the adsorption of heavy metal ions.

Desorption ability of CNF/PVA/PEI nanoparticle

In addition to desired removal rate, ideal environmental remediation materials should possess excellent regeneration and recyclability (Fig.6). The Cu^{2+} removal rate of CNF/PVA/PEI nanoparticle remained to 80% after three adsorption-desorption cycles. The removal rate was decreased slightly with the cycle time, which was due to the decrease of effective adsorption sites in CNF/PVA/PEI nanoparticle. There were two reasons to result in the reduction of removal rate. One of that was Cu^{2+} combined with some active sites of CNF/PVA/PEI nanoparticle with an irreversible way. The other one was due to a few amine groups were protonated during the desorption process (Tang et al. 2020b).

Comparison with reported studies

The final adsorption properties of CNF/PVA/PEI nanoparticle were evaluated and are presented in Table 3 for comparison with reported data. The CNF/PVA/PEI nanoparticle reached adsorption equilibrium within one hour, far better than the 2,3-dialdehyde nano-fibrillated celluloses (DNFCs)(Lei et al. 2019) and the perlite/solid iron(Khudr et al. 2021). The removal rate of CNF/PVA/PEI nano reached 93% in the solution of 20-80mg/ L Cu^{2+} solution, far higher than the perlite/solid iron. It is worth noting that, the removal rate can still reach 80% after three cycles, However, DNFCS, Perlite/ Solid Ion, Multi-walled Carbon Nanotubes (MWCNT) do not show cyclic performance(Mobasherpour et al. 2014). Which means CNF/PVA/PEI nanoparticle may be an excellent alumina bent can be applied in practical application. The adsorption capacity of CNF/PVA/PEI nanoparticles displayed improved significantly is superior than other samples (Table 3).

Conclusion

To improve the removal rate and adsorption capability of CNF based adsorbents for Cu^{2+}, we introduce a novel and green approach to assemble CNF/PVA/PEI nanoparticle, which reaches fast adsorption of Cu^{2+}. Its adsorption for Cu^{2+} is very consistent with the pseudo-second-order model among four kinds of adsorption models. It is evident that the chemical adsorption is the main rate-limiting step when the CNF based adsorbent is carried out to remove Cu^{2+} in water. We can assemble the environmentally friendly and effective CNF based adsorbents for the removal of Cu^{2+} by doping new chemical agents and controlling the structure in the near future. Overall, this study not only reveals adsorption mechanism of CNF/PVA/PEI nanoparticle for Cu^{2+} removal, but also provides a promising pathway to regulate the CNF based adsorbents for the removal of the other heavy metal ions in water.

Declarations

Authors' contribution All authors contributed as the main contributors of this work. All authors performed the literature search and analysis. All authors had drafted, revised the work and approved the final paper.

Funding This article was financially supported by the National Key R&D Program of China(2017YFB0307900).

Availability of data and material Not applicable.

Code availability Not applicable.

Compliance with ethical standards

Conflict of interest The authors declare that they have no conflict of interest.

Ethical approval This article does not contain any studies with human participants or animals performed by any of the authors.

References

1. A XJ, A ZX, B QL, B YC, A FL (2017) Polyethyleneimine-bacterial cellulose bioadsorbent for effective removal of copper and lead ions from aqueous solution Bioresource Technology 244:844-849 doi:10.1016/j.biortech.2017.08.072
2. Anirudhan TS, Shainy F, Deepa JR (2019) Effective removal of Cobalt(II) ions from aqueous solutions and nuclear industry wastewater using sulfhydryl and carboxyl functionalised magnetite nanocellulose composite: batch adsorption studies Chem Ecol 35:235-255 doi:10.1080/02757540.2018.1532999
3. Du HS et al. (2016) Preparation and characterization of thermally stable cellulose nanocrystals via a sustainable approach of FeCl3-catalyzed formic acid hydrolysis Cellulose 23:2389-2407 doi:10.1007/s10570-016-0963-5
4. Eun S, Hong HJ, Kim H, Jeong HS, Kim S, Jung J, Ryu J (2020) Prussian blue-embedded carboxymethyl cellulose nanofibril membranes for removing radioactive cesium from aqueous solution Carbohydrate Polymers 235 doi:10.1016/j.carbpol.2020.115984
5. Fu F, Wang Q (2011) Removal of heavy metal ions from wastewaters: a review Journal of Environmental Management 92:407-418 doi:10.1016/j.jenvman.2010.11.011
6. Garba ZN, Lawan I, Zhou W, Zhang M, Wang L, Yuan ZJTSotTE (2020) Microcrystalline cellulose (MCC) based materials as emerging adsorbents for the removal of dyes and heavy metals - A review Science of the Total Environment 717 doi:10.1016/j.scitotenv.2019.135070
7. Islam MS, Sharif SB, Lee JJL, Habiba U, Afifi AM (2017) Adsorption of divalent heavy metal ion by mesoporous-high surface area chitosan/poly (ethylene oxide) nanofibrous membrane Carbohydrate Polymers 157:57-64 doi:10.1016/j.carbpol.2016.09.063
8. Jordan JH, Easson MW, Condon BD (2019) Alkali Hydrolysis of Sulfated Cellulose Nanocrystals: Optimization of Reaction Conditions and Tailored Surface Charge Nanomaterials 9:15 doi:10.3390/nano9091232
9. Khudr MS, Ibrahim YME, Garforth A, Alfutimie A (2021) On copper removal from aquatic media using simultaneous and sequential iron-perlite composites J Water Process Eng 40:6 doi:10.1016/j.jwpe.2020.101842

10. Lei Z, Gao W, Zeng J, Wang B, Xu JJCP (2019) The mechanism of Cu (II) adsorption onto 2,3-dialdehyde nano-fibrillated celluloses Carbohydrate Polymers 230 doi:10.1016/j.carbpol.2019.115631
11. Mo L (2019) 3D multi-wall perforated nanocellulose-based polyethylenimine aerogels for ultrahigh effcient and reversible removal of Cu(2+) ions from water Chemical Engineering Journal 378 doi:10.1016/j.cej.2019.122157
12. Mobasherpour I, Salahi E, Ebrahimi M (2014) Thermodynamics and kinetics of adsorption of Cu(II) from aqueous solutions onto multi-walled carbon nanotubes J Saudi Chem Soc 18:792-801 doi:10.1016/j.jscs.2011.09.006
13. Niu X, Liu YT, Fang GG, Huang CB, Rojas OJ, Pan H (2018) Highly Transparent, Strong, and Flexible Films with Modified Cellulose Nanofiber Bearing UV Shielding Property Biomacromolecules 19:4565-4575 doi:10.1021/acs.biomac.8b01252
14. Pal A, Majumder K, Sengupta S, Das T, Bandyopadhyay A (2017) Adsorption of soluble Pb(II) by a photocrosslinked polysaccharide hybrid: A swelling-adsorption correlation study Carbohydrate Polymers 177:144-155 doi:10.1016/j.carbpol.2017.08.122
15. Qin H, Hu T, Zhai Y, Lu N, Aliyeva J (2019) The improved methods of heavy metals removal by biosorbents: A review Environmental Pollution 258 doi:10.1016/j.envpol.2019.113777
16. Qin ZY, Tong GL, Chin YCF, Zhou JC (2011) Preparation of Ultrasonic-assisted high carboxylate content cellulose nanpcrystals by TEMPO oxidation Bioresources 6:1136-1146
17. Rani MSA, Rudhziah S, Ahmad A, Mohamed NS (2014) Biopolymer Electrolyte Based on Derivatives of Cellulose from Kenaf Bast Fiber Polymers 6:2371-2385 doi:10.3390/polym6092371
18. Shao et al. (2017) Soy protein-based polyethylenimine hydrogel and its high selectivity for copper ion removal in wastewater treatment JOURNAL OF MATERIALS CHEMISTRY A 5:4163-4171 doi:10.1039/c6ta10814h
19. Silva NHCS, Figueira P, Fabre E, Pinto RJB, Polymers CSRFJC (2020) Dual nanofibrillar-based bio-sorbent films composed of nanocellulose and lysozyme nanofibrils for mercury removal from spring waters Carbohydrate Polymers 238:116210
20. Sirvio, JA, Visanko, CHEM LJG (2015) Deep eutectic solvent system based on choline chloride-urea as a pre-treatment for nanofibrillation of wood cellulose Green Chem 17:3401-3406 doi:10.1039/c5gc00398a
21. Stern BR (2010) Essentiality and Toxicity in Copper Health Risk Assessment: Overview, Update and Regulatory Considerations J Toxicol Env Health Part A 73:114-127 doi:10.1080/15287390903337100
22. Takeno H, Inoguchi H, Hsieh WC (2020) Mechanical and structural properties of cellulose nanofiber/poly(vinyl alcohol) hydrogels cross-linked by a freezing/thawing method and borax Cellulose 27:4373-4387 doi:10.1007/s10570-020-03083-z
23. Tang CX, Brodie P, Li YZ, Grishkewich NJ, Brunsting M, Tam KC (2020a) Shape recoverable and mechanically robust cellulose aerogel beads for efficient removal of copper ions Chemical

Engineering Journal 392:11 doi:10.1016/j.cej.2020.124821

24. Tang F et al. (2020b) Green acid-free hydrolysis of wasted pomelo peel to produce carboxylated cellulose nanofibers with super absorption/flocculation ability for environmental remediation materials Chemical Engineering Journal 395 doi:10.1016/j.cej.2020.125070
25. Tarchoun AF, Trache D, Klapotke TM, Derradji M, Bessa W (2019) Ecofriendly isolation and characterization of microcrystalline cellulose from giant reed using various acidic media Cellulose 26:7635-7651 doi:10.1007/s10570-019-02672-x
26. Uddin MK (2017) A review on the adsorption of heavy metals by clay minerals, with special focus on the past decade Chemical Engineering Journal 308:438-462 doi:10.1016/j.cej.2016.09.029
27. Wan Ngah WS, Hanafiah MA (2008) Removal of heavy metal ions from wastewater by chemically modified plant wastes as adsorbents: a review Bioresour Technol 99:3935-3948 doi:10.1016/j.biortech.2007.06.011
28. Wang X et al. (2019) Facile Fabrication of Superhydrophobic and Eco-Friendly Polylactic Acid Foam for Oil-Water Separation via Skin-Peeling Acs Applied Materials Interfaces 14362-14367 doi:10.1021/acsami.9b02285
29. Yao QF, Fan BT, Xiong Y, Jin CD, Sun QF, Sheng CM (2017) 3D assembly based on 2D structure of Cellulose Nanofibril/Graphene Oxide Hybrid Aerogel for Adsorptive Removal of Antibiotics in Water Sci Rep 7:13 doi:10.1038/srep45914
30. Zhang N, Zang G-L, Shi C, Yu H-Q, Sheng G-PJJoHM (2016) A novel TEMPO-mediated oxidized cellulose nanofibrils modified with PEI: Preparation, characterization, and application for Cu(II) removal J Hazard Mater 316:11-18 doi:10.1016/j.jhazmat.2016.05.018
31. Zheng QF, Cai ZY, Gong SQ (2014) Green synthesis of polyvinyl alcohol (PVA)-cellulose nanofibril (CNF) hybrid aerogels and their use as superabsorbents Journal of Materials Chemistry A 2:3110-3118 doi:10.1039/c3ta14642a
32. Zhu YC, Wu CJ, Yu DM, Ding QJ, Li RG (2021) Tunable micro-structure of dissolving pulp-based cellulose nanofibrils with facile prehydrolysis process Cellulose 28:3759-3773 doi:10.1007/s10570-021-03760-7

Tables

Table 1 Thermal stability parameters of Cellulose, CNF, CNF/PVA aerogel, CNF/PVA/PEI nanoparticle.

Sample	Cellulose	CNF	CNF/PVA	CNF/PVA/PEI
T_0(°C)	269.8	168.2	177.6	194.9
$T_{5\%}$(°C)	294.1	207.1	221.8	216.4
T_{max}(°C)	384.9	312.7	324.7	327.5

[a]T_0, $T_{5\%}$, T_{max} were calculated from TGA curves.

Table 2 Specific surface area and average pore size of CNF, CNF/PVA aerogel, CNF/PVA/PEI nanoparticle

Sample	BET surface area (m^2/g)	Langmuir surface aera (m^2/g)	Pore size(Å)
CNF/PVA Aerogel	56.37	307.81	55.15
CNF/PVA/PEI Nanoparticle	22.93	183.61	85.67

Table 3 Comparison of adsorption capacity of different adsorption materials

Adsorbent	Adsorption equilibrium	Adsorption capacity	Remove rate	Cycles times	Ref
DNFCs	8h	29.52mg/g		/	(Lei et al. 2019)
Perlite/solid iron	2h	/	17.6mg/L,71%	/	(Khudr et al. 2021)
MWCNT	0.5h	12.34mg/g		/	(Mobasherpour et al. 2014)
CNF/PVA/PEI nanoparticle	1h	/	20-80mg/L,>93%	3	This work

Table 4 The fitting parameters of adsorption kinetics of Cu^{2+}

Models	Parameters	Concentration（mg/L）			
		20	40	60	80
Pseudo-first-order	$K_1/(min^{-1})$	-0.07115	-0.05069	-0.04057	-0.03465
	R^2	0.9159	0.9102	0.9006	0.9677
Pseudo-second-order	K_2/(g/mg*min)	0.10022	0.05098	0.03394	0.02432
	R^2	0.9906	0.9994	0.9997	0.9971
Elovich equation	K_e	2.04691	1.64042	2.84893	6.93541
	C	0.30178	12.24967	15.92302	6.6082
	R^2	0.8617	0.8065	0.9048	0.9594
Intra-particle diffusion	K_i	0.57017	0.44114	0.82202	2.02043
	A	3.96947	15.39234	20.87333	18.38915
	R^2	0.6922	0.5616	0.7609	0.8709

Figures

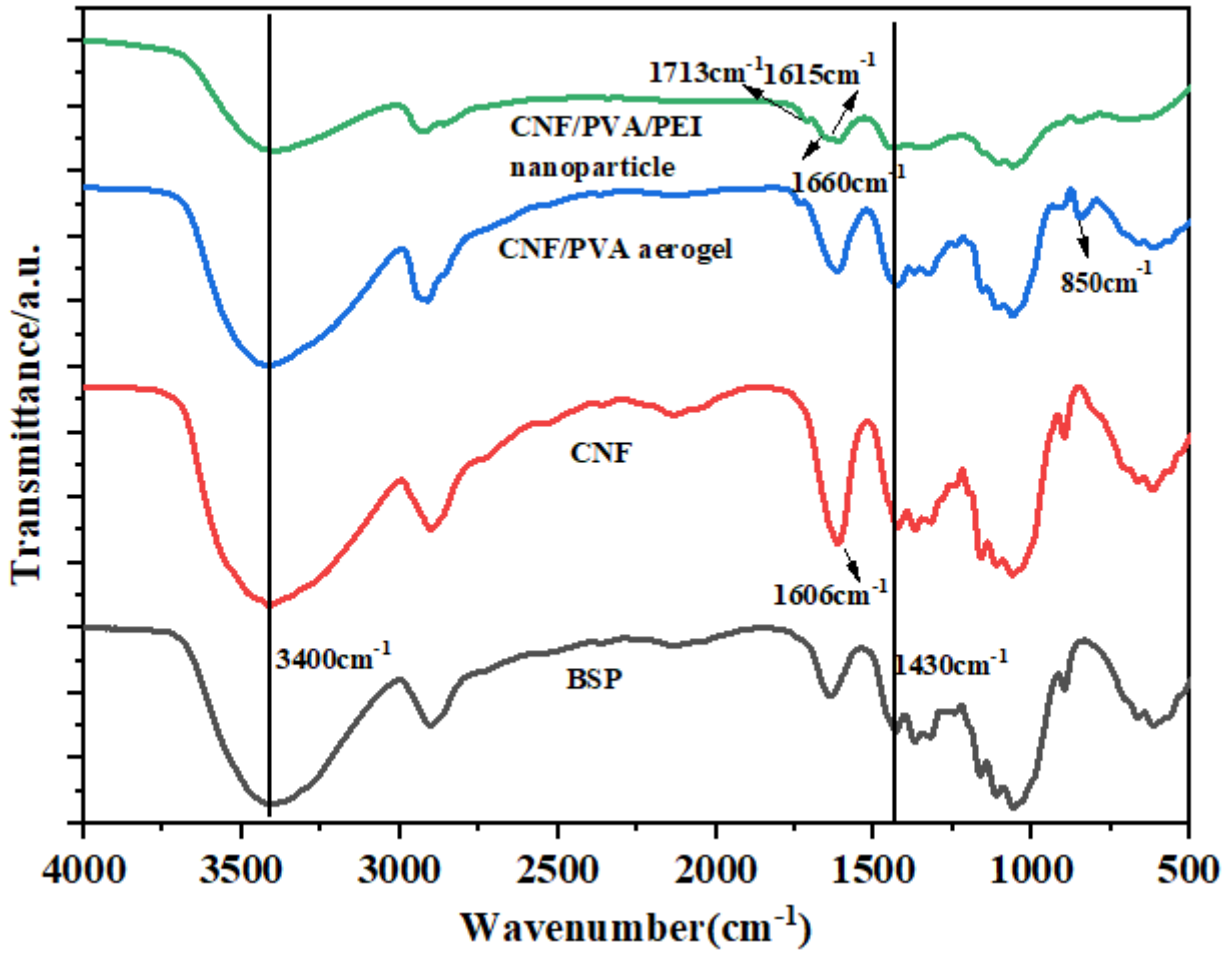

Figure 1

FTIR analysis of BSP, CNF, CNF/PVA aerogel, CNF/PVA/PEI nanoparticle

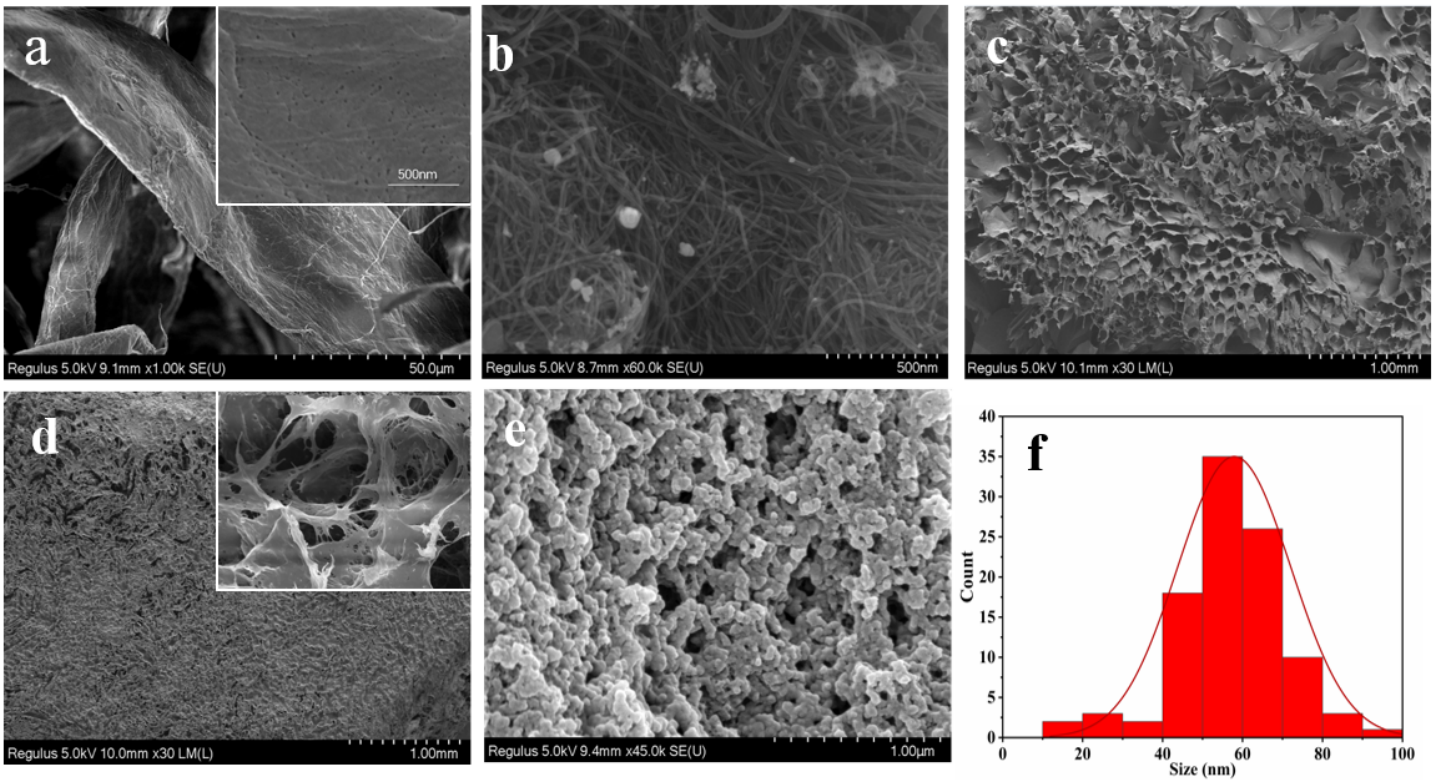

Figure 2

SEM images of a BSP, b CNF, c CNF aerogel, d CNF/PVA aerogel, e CNF/PVA/PEI nanoparticle, f Particle size distribution of CNF/PVA/PEI nanoparticle

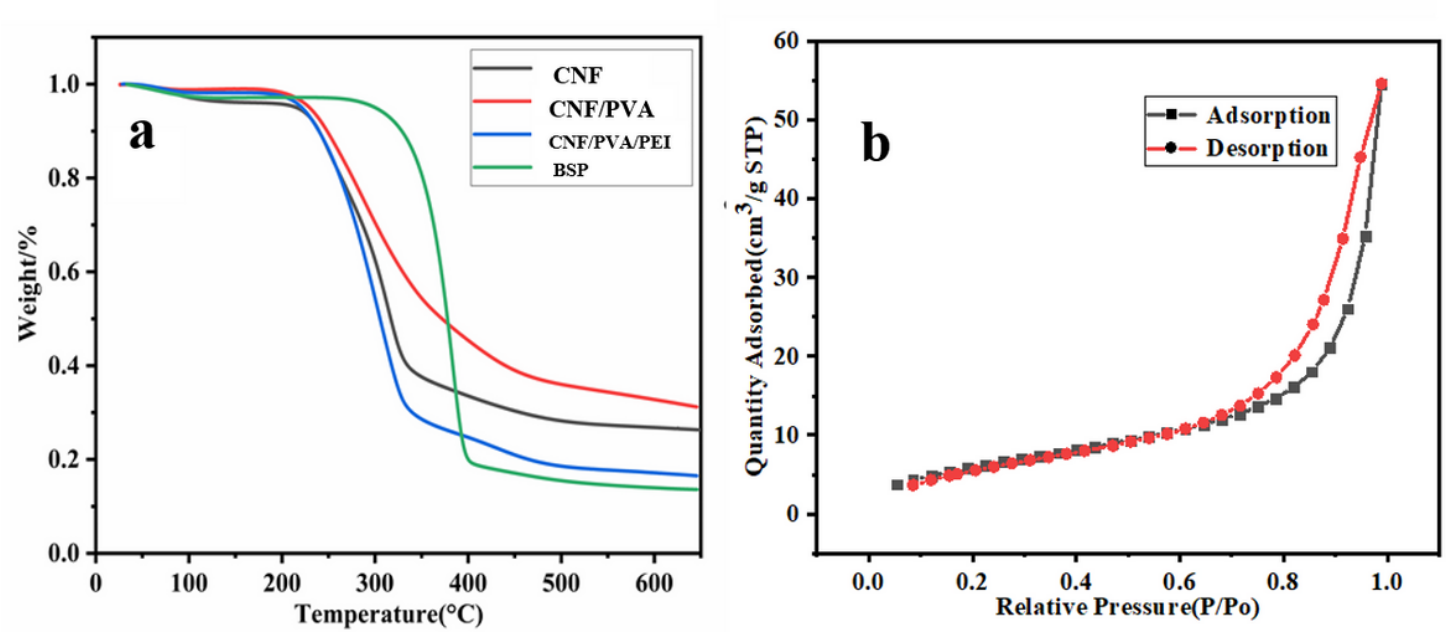

Figure 3

(a) TGA for BSP, CNF, CNF/PVA aerogel, CNF/PVA/PEI nanoparticle. (b) Adsorption-desorption isotherm and pore size distribution of CNF/PVA/PEI nanoparticle at 77K

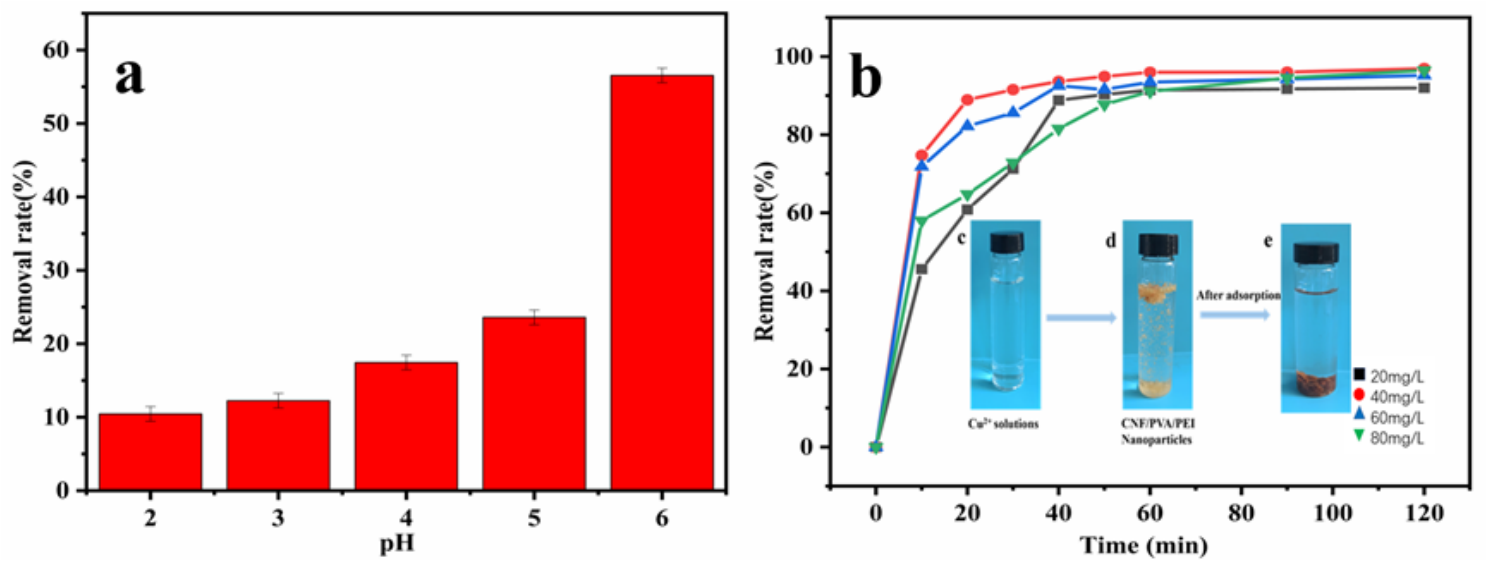

Figure 4

(a)Effect of initial pH on the adsorption of Cu2+ onto CNF/PVA/PEI nanoparticle. (b) The removal rate of CNF/PVA/PEI nanoparticle at the concentration of 20, 40, 60, 80 mg/L. (c-e) Photographs of the CNF/PVA/PEI nanoparticle being inserted into the Cu2+-contaminated deionized water

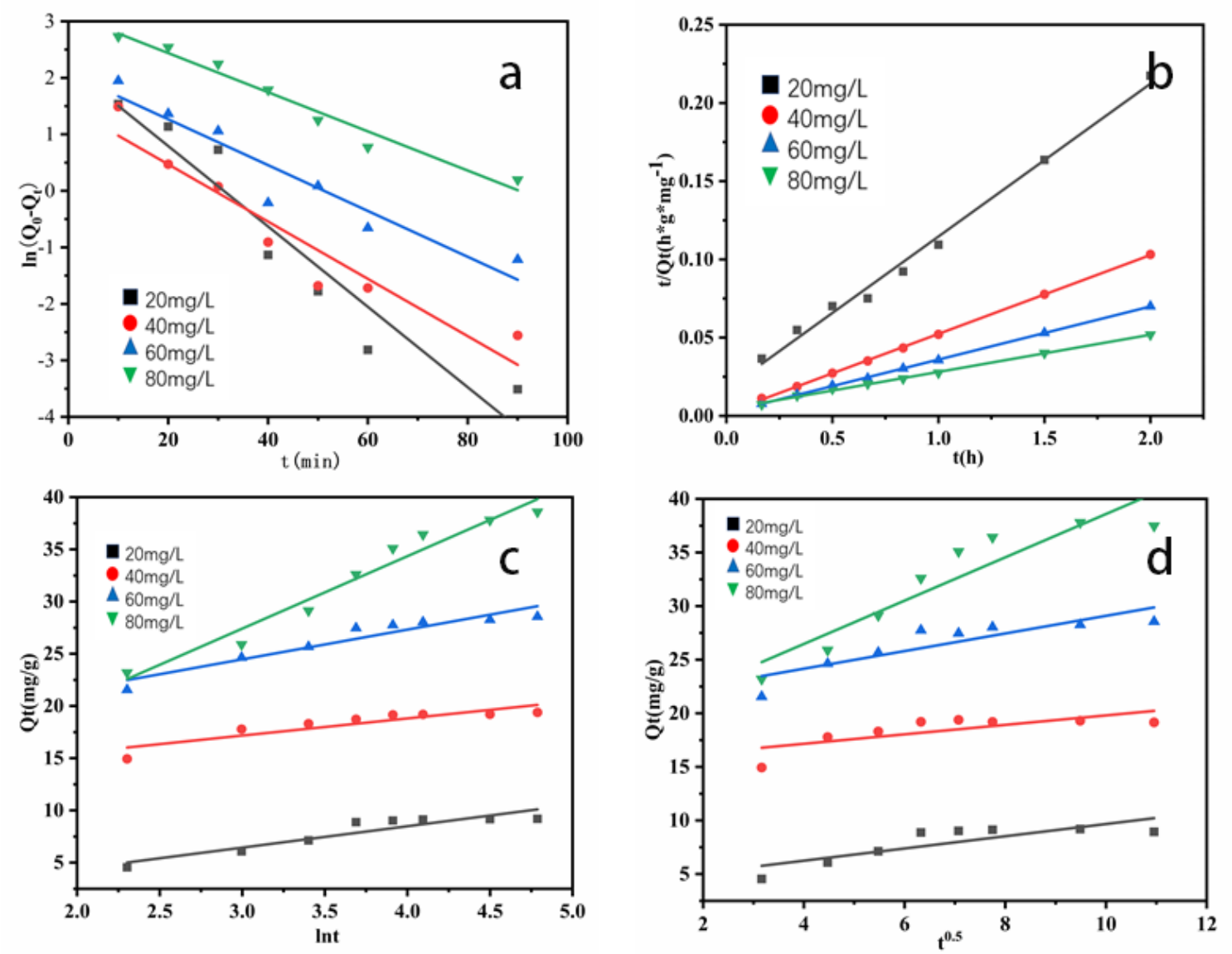

Figure 5

(a) Plots of Pseudo-first-order, (b) Pseudo-second-order, (c) Elovich, (d) Intra-particle diffusion models of 20, 40, 60, 80mg/L

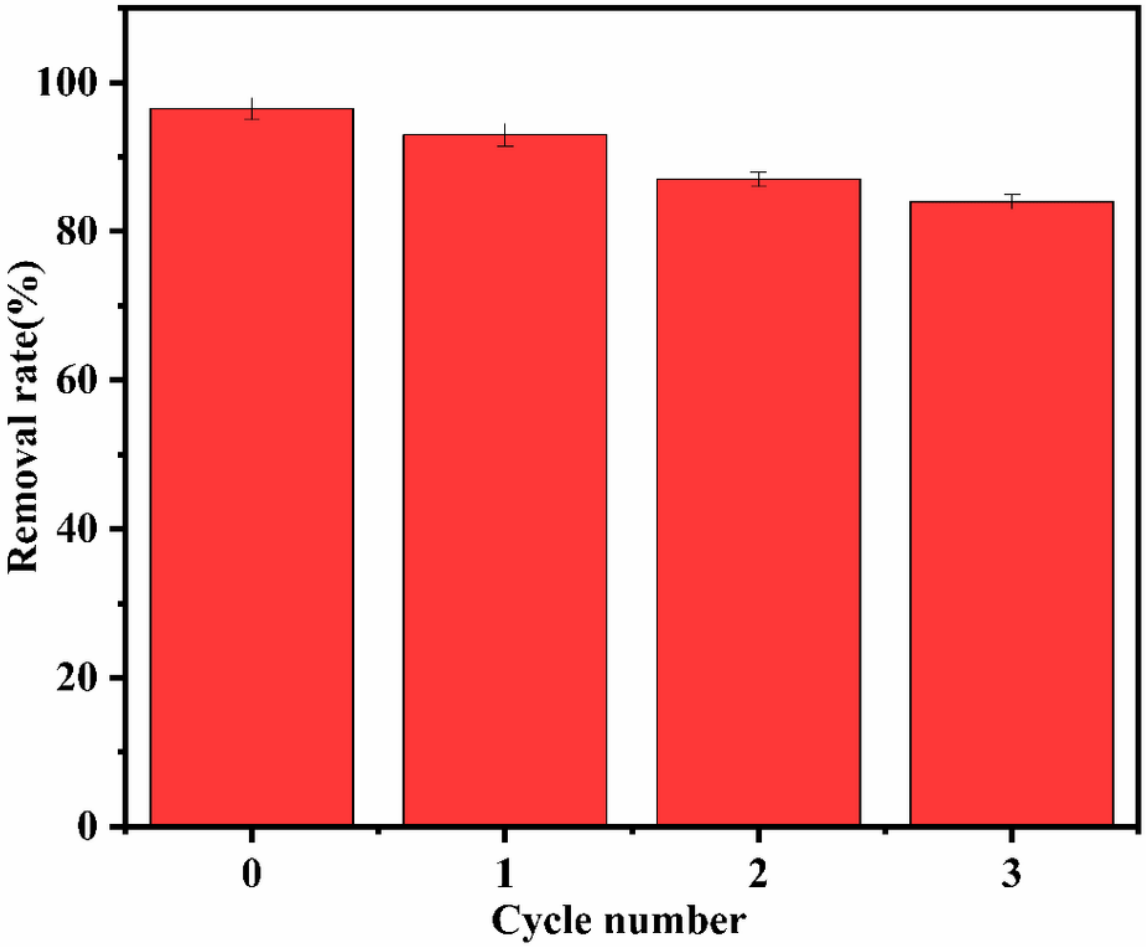

Figure 6

Recycling performance of CNF/PVA/PEI nanoparticle for Cu2+ adsorption

Supplementary Files

This is a list of supplementary files associated with this preprint. Click to download.

- GraphicalAbstract.jpg
- renamed25c40.docx